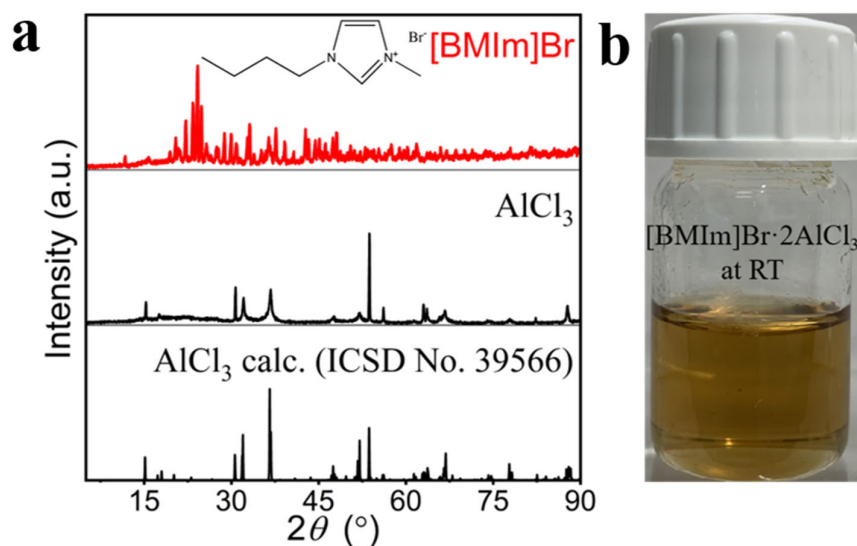


## Supplementary Materials

### A stable porous aluminum electrode with high capacity for rechargeable lithium-ion batteries

Peng Chen and Michael Ruck



**Figure S1.** (a) The comparison of the [BMIm]Br and AlCl<sub>3</sub> used in this paper with the standard XRD patterns (the insertion is the molecular structure of [BMIm]Br). (b) Photograph of the IL [BMIm]Br·2AlCl<sub>3</sub> at room temperature.

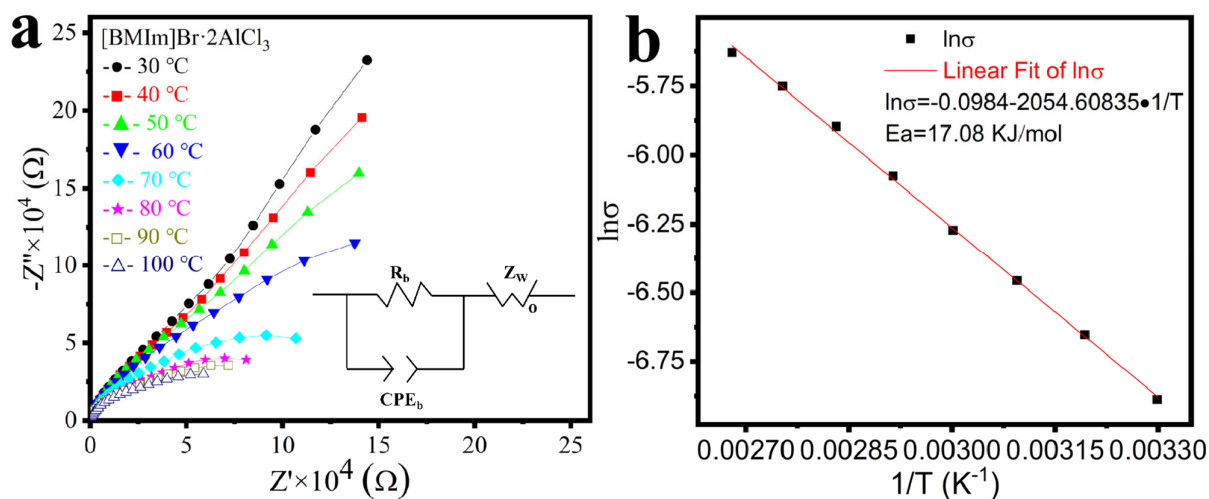


**Figure S2.** (a) EIS of the IL [BMIm]Br·2AlCl<sub>3</sub> (inset: the equivalent circuit for the simulation). (b) The linear fitting curve of activation energy.

**Table S1.** Measured data and corresponding calculated values of ionic conductivity of the IL [BMIm]Br·2AlCl<sub>3</sub>.

Temperature/°C	Thickness/mm	Impedance/ $\Omega$	Area/cm <sup>2</sup>	Ionic Conductivity/(S cm <sup>-1</sup> )
30	3.03	95.03	3.14	$1.02 \cdot 10^{-3}$
40	3.03	74.59	3.14	$1.29 \cdot 10^{-3}$
50	3.03	61.38	3.14	$1.57 \cdot 10^{-3}$
60	3.03	51.05	3.14	$1.89 \cdot 10^{-3}$
70	3.03	41.98	3.14	$2.30 \cdot 10^{-3}$
80	3.03	35.16	3.14	$2.75 \cdot 10^{-3}$
90	3.03	30.33	3.14	$3.18 \cdot 10^{-3}$
100	3.03	26.94	3.14	$3.59 \cdot 10^{-3}$

Equations for the temperature dependence of the ionic conductivity:

$$\sigma(T) = A \cdot \exp\left(\frac{-E_a}{R \cdot T}\right) \quad (\text{S1})$$

$$\ln(\sigma(T)) = \ln(A) - \frac{E_a}{R \cdot T} \quad (\text{S2})$$

$$\ln(\sigma(T)) = \ln(A) - \frac{E_a}{R} \cdot \frac{1}{T} \quad (\text{S3})$$

where  $\sigma$  is the ionic conductivity,  $T$  is the absolute temperature,  $E_a$  is the activation energy, and  $A$  is a pre-exponential factor.

**Table S2.** Based on the calculated ionic conductivity ( $\sigma$ ) of the IL [BMIm]Br·2AlCl<sub>3</sub>, the relevant parameters used to fit the activation energy  $E_a$  are calculated according to the Equations S1–S3.

$T / ^\circ\text{C}$	$\sigma / (\text{S cm}^{-1})$	$\ln \sigma$	$T^{-1} / (10^{-3} \text{ K}^{-1})$
30	$1.02 \cdot 10^{-3}$	-6.89	3.30
40	$1.29 \cdot 10^{-3}$	-6.65	3.19
50	$1.57 \cdot 10^{-3}$	-6.46	3.09
60	$1.89 \cdot 10^{-3}$	-6.27	3.00
70	$2.30 \cdot 10^{-3}$	-6.07	2.91
80	$2.75 \cdot 10^{-3}$	-5.90	2.83
90	$3.18 \cdot 10^{-3}$	-5.75	2.75
100	$3.59 \cdot 10^{-3}$	-5.63	2.68

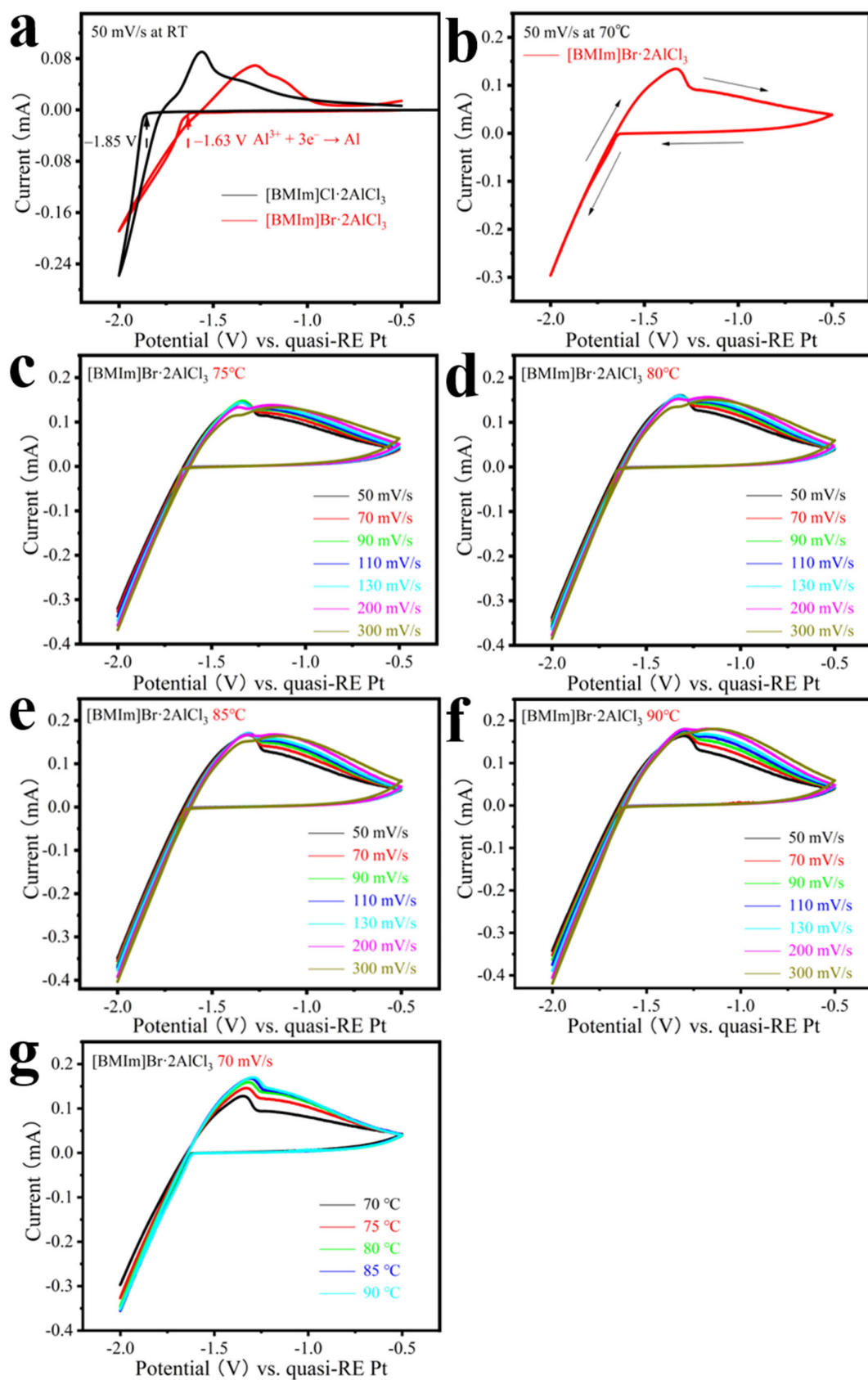


**Figure S3.** Synopsis of the CVs of [BMIm]Br·2AlCl<sub>3</sub> and [BMIm]Cl·2AlCl<sub>3</sub> at different scan rates and temperatures.

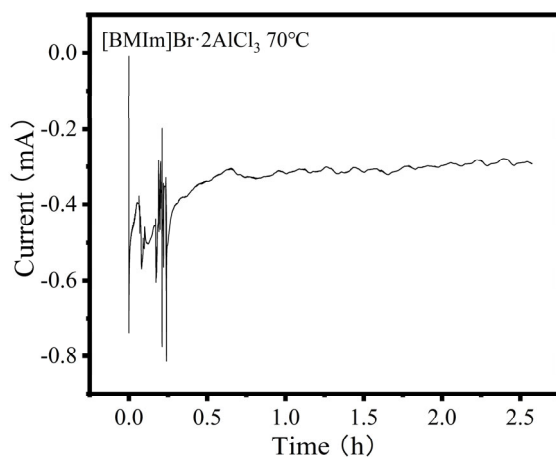


**Figure S4.** Time–current curve via potentiostatic electrolysis for electrodeposited Al at  $-1.70$  V and  $70$  °C after about 2.5 h.

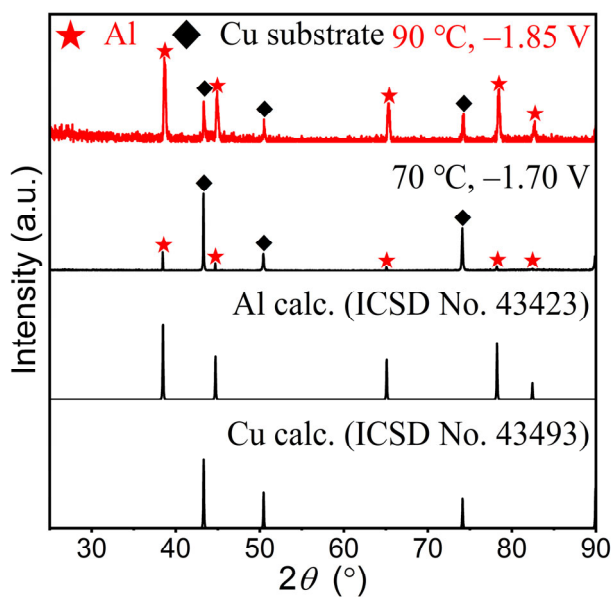


**Figure S5.** PXRD pattern of Al electrodeposited on Cu foil from of the IL  $[\text{BMIm}]\text{Br} \cdot 2\text{AlCl}_3$  at chosen conditions.



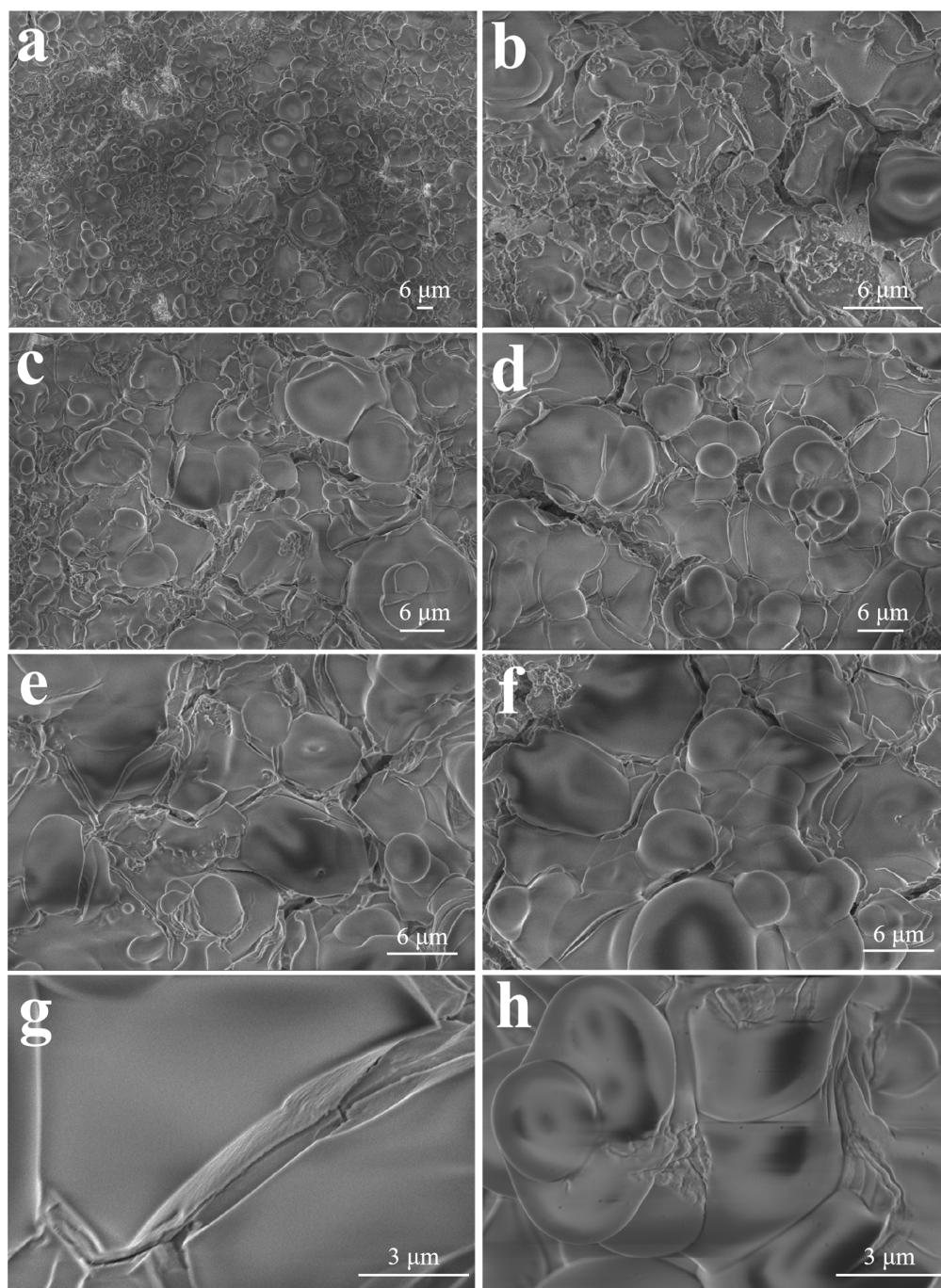


**Figure S6. (a–h)** SEM images (increasing magnification) of electrodeposited Al on Cu foil substrate at  $-1.70$  V and  $70$  °C after about 2.5 h.

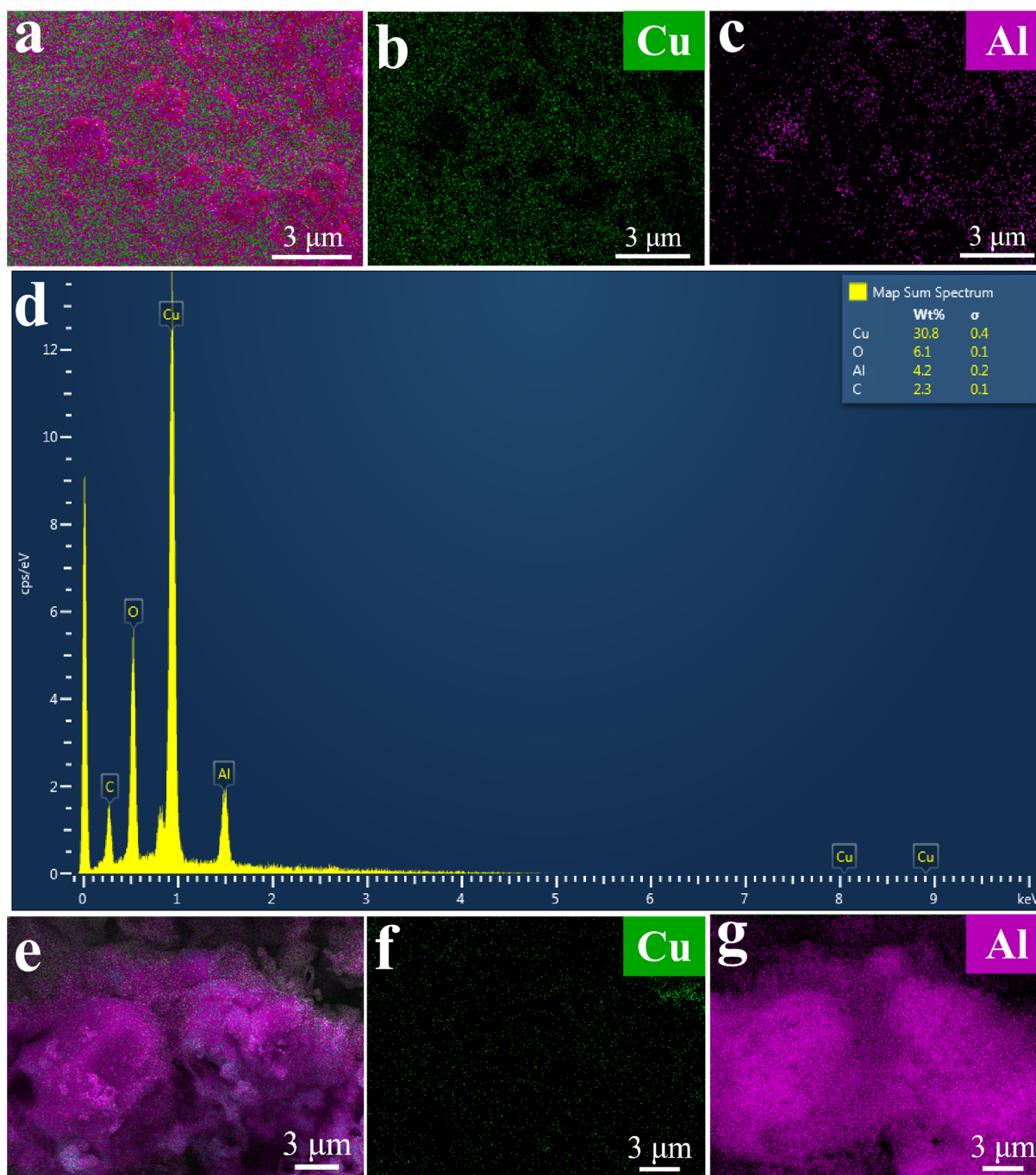


**Figure S7.** EDX mappings and signals of all elements of the Cu and Al distribution of the Al layer electrodeposited at  $-1.70$  V (**a-d**) or  $-1.85$  V (**e-g**) at  $70$  °C.

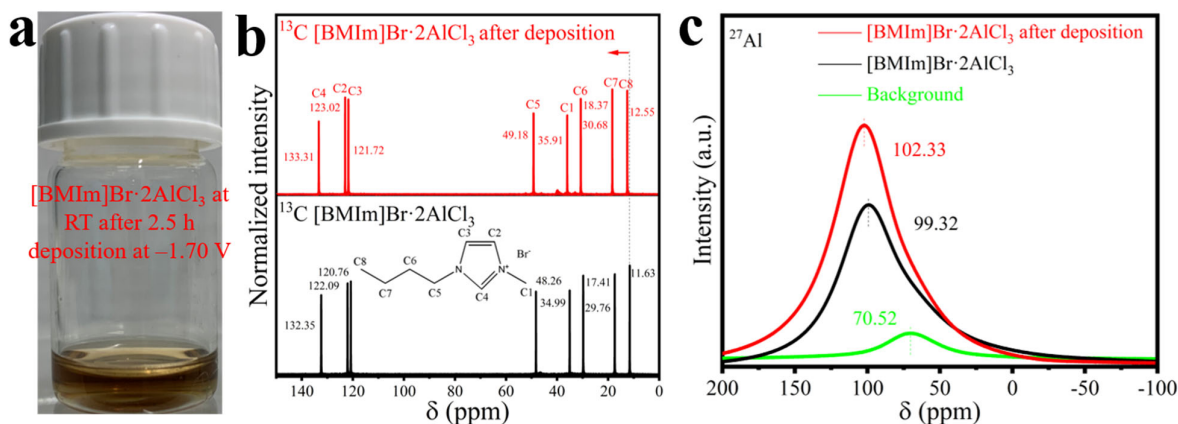


**Figure S8.** (a) Photograph of the [BMIm]Br·2AlCl<sub>3</sub> solution at room temperature after about 2.5 h of Al electrodeposition at -1.70 V and 70 °C. Comparison of pristine [BMIm]Br·2AlCl<sub>3</sub> (black line) and the ILs after about 2.5 h of Al electrodeposition at -1.70 V and 70 °C (red line). (b) Corresponding <sup>13</sup>C NMR spectra (the insertion is the labeling of different carbon atoms of [BMIm]Br). (c) <sup>27</sup>Al NMR spectra.

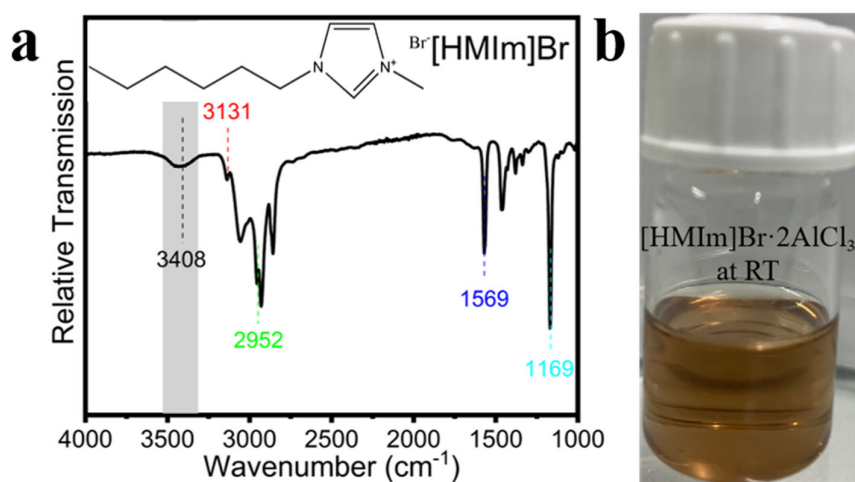


**Figure S9.** (a) FT-IR spectrum in the range of  $1000\text{ cm}^{-1} \leq \tilde{\nu} \leq 4000\text{ cm}^{-1}$  of [HMIm]Br used in this paper (the insertion is the molecular structure of [HMIm]Br). (b) Photograph of [HMIm]Br·2AlCl<sub>3</sub> ILs solution at room temperature.



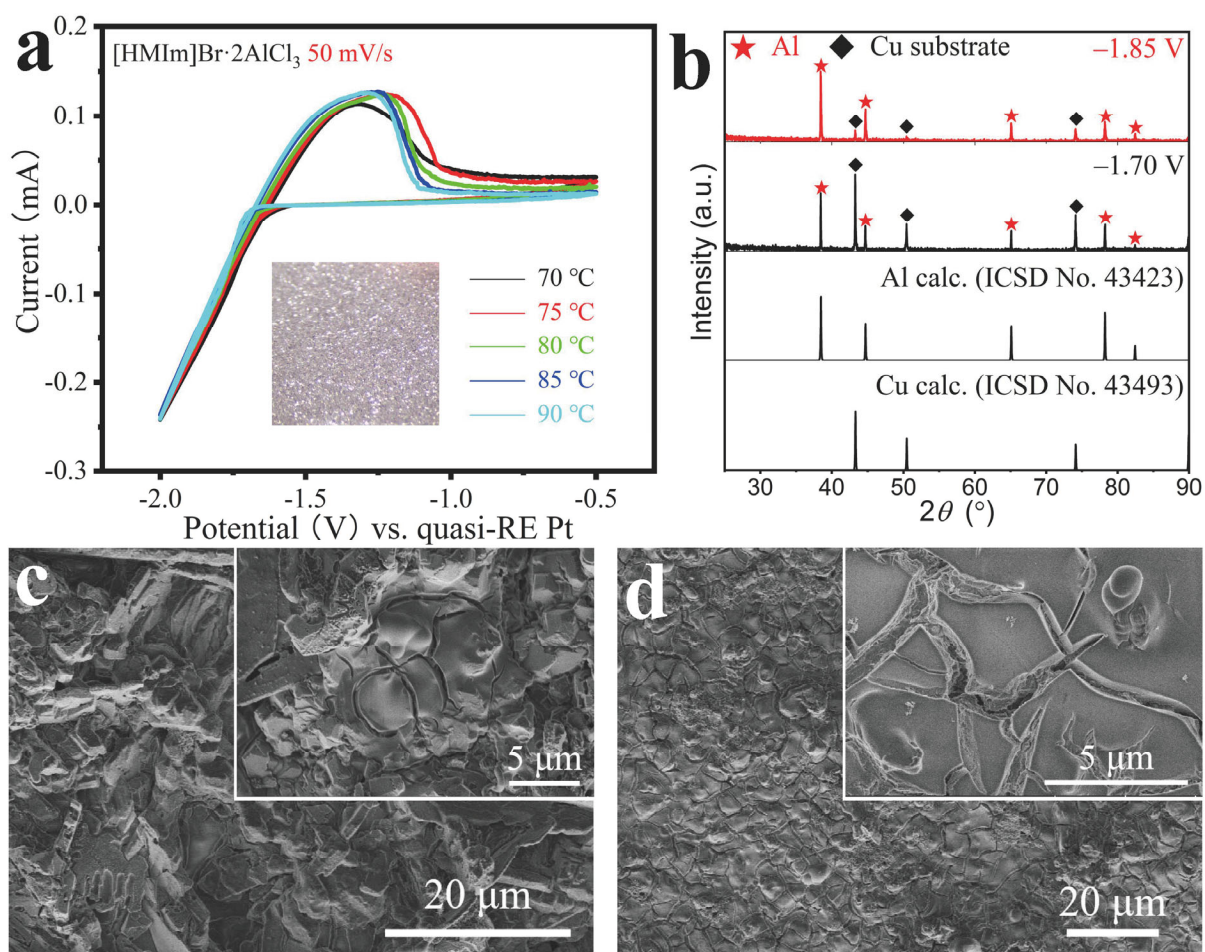


**Figure S10.** (a) CV of  $[\text{HMIIm}]\text{Br} \cdot 2\text{AlCl}_3$  at a scan rate of  $50 \text{ mV s}^{-1}$  and different temperatures; inset: photograph of the Cu foil substrate after 7 h of Al electrodeposition at  $-1.70 \text{ V}$  and  $90^\circ\text{C}$ . (b) Comparison of the PXRD pattern of the coated electrode. SEM images of the Al layers with enlarged details (inset) that were electrodeposited at (c)  $-1.70 \text{ V}$  or (d)  $-1.85 \text{ V}$  at  $90^\circ\text{C}$  within 7 h.

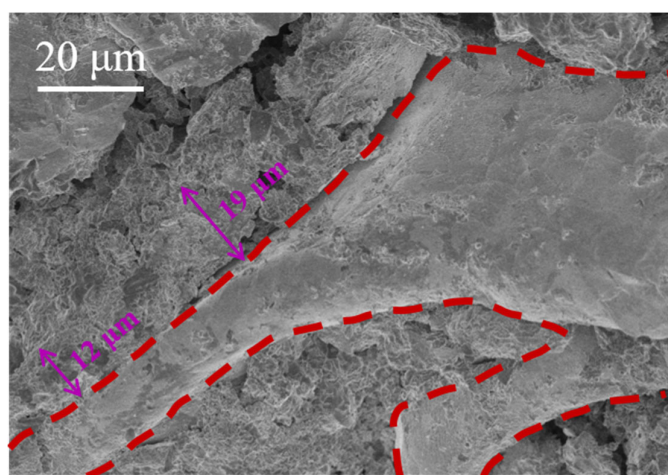


**Figure S11.** Cross-sectional SEM image of the Al layer electrodeposited at  $-1.85 \text{ V}$  and  $90^\circ\text{C}$  (skeleton structure of  $^{3\text{D}}\text{Cu}$  indicated with red dotted lines, the thickness of Al layer is about  $12\text{--}19 \mu\text{m}$ ).

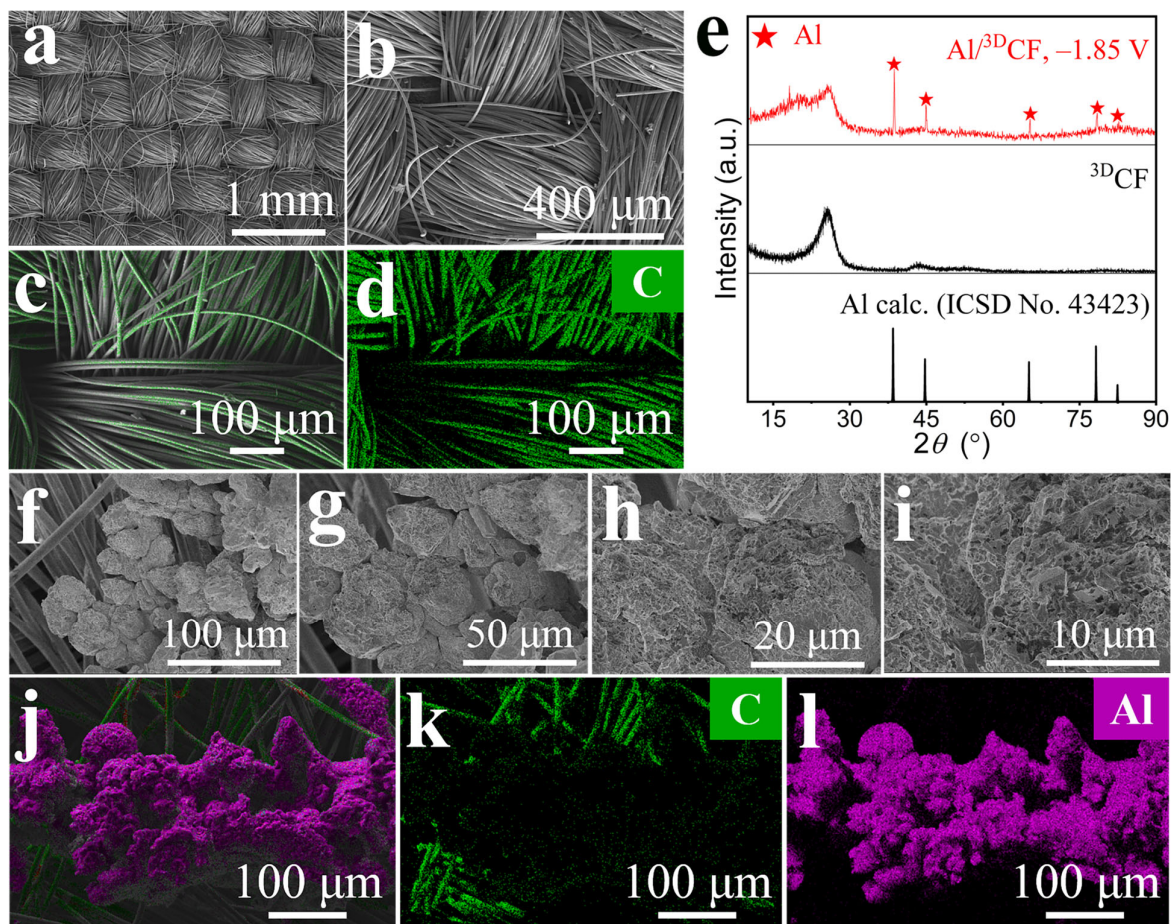


**Figure S12.** (a-b) SEM images and (c-d) EDX mappings of all elements of the C distribution of  ${}^3\text{D}\text{CF}$ . (e) PXRD pattern comparison. (f-i) SEM images and (j-l) EDX mappings of all elements of the C and Al distribution of the loaded  $\text{Al}/{}^3\text{D}\text{CF}$  electrode electrodeposited at  $-1.85\text{ V}$  at  $90\text{ }^\circ\text{C}$ .

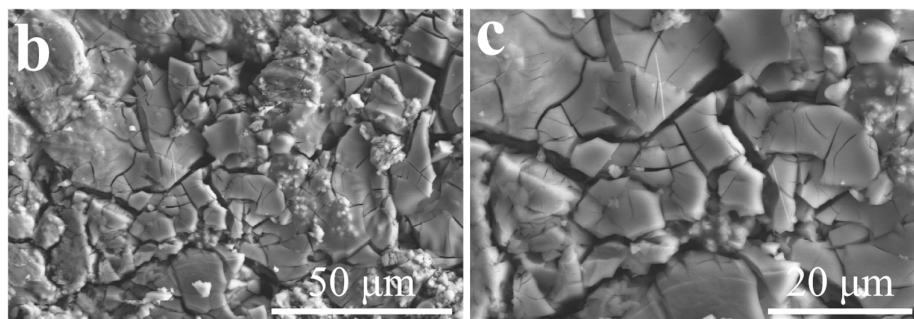
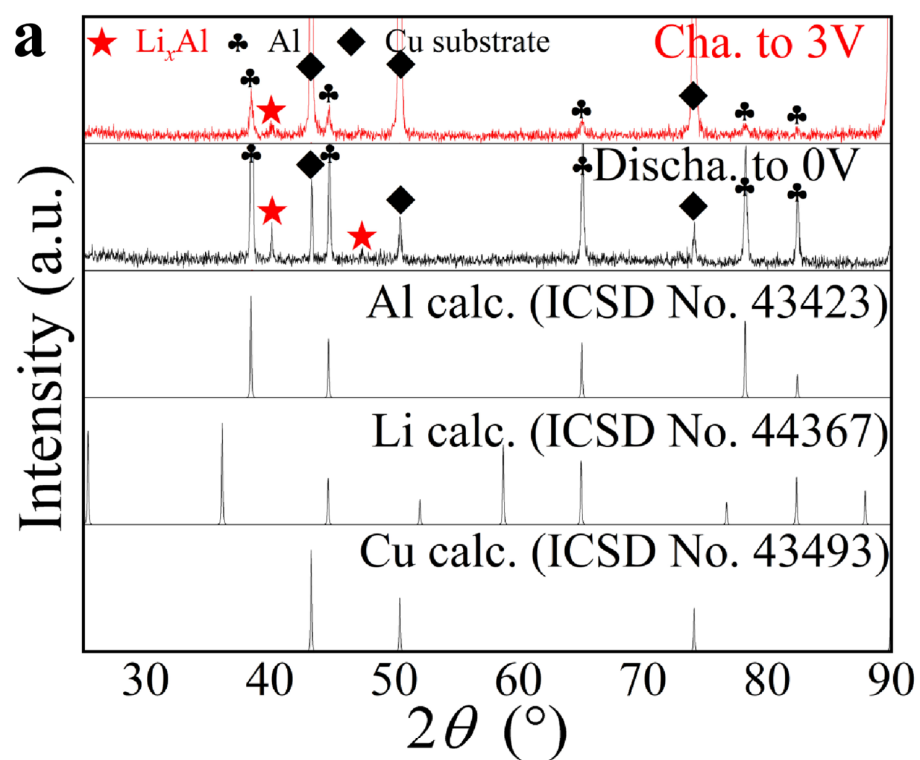


**Figure S13.** (a) PXRD pattern comparison of discharged to 0 V at  $4.2 \text{ mA g}^{-1}$  and charged to 3 V electrode at  $21 \text{ mA g}^{-1}$ . (b-c) SEM images (increasing magnification) of an  $\text{Al}/^{3\text{D}}\text{Cu}$  electrode charged to 3 V at  $21 \text{ mA g}^{-1}$ .